CONF-950908--8

SEALANT MATERIALS FOR SOLID OXIDE FUELS AND OTHER HIGH-TEMPERATURE CERAMICS*

Timothy W. Kueper and Ira D. Bloom

Electrochemical Technology Program
Chemical Technology Division
Argonne National Laboratory
9700 South Cass Avenue
Argonne, Illinois 60439

To be presented at
2nd International Conference on Heat Resistant Materials
Gatlinburg, Tennessee

September 11-14, 1995

*This work was done under the auspices of the U.S. Department of Energy, Morgantown Energy Technology Center, under contract number W 31-109-Eng-38.

Sealant Materials for Solid Oxide Fuel Cells and Other High-Temperature Ceramics

Timothy W. Kueper and Ira D. Bloom
Electrochemical Technology Program
Chemical Technology Division
Argonne National Laboratory

Abstract

Glass-ceramic sealing materials have been developed with mechanical and chemical properties suitable for a variety of high-temperature applications. We have demonstrated the ability to tailor the thermal expansion coefficient between 8 and 12 × 10^{-6}/°C, and the softening temperature can be adjusted such that the materials have suitable viscosities for a soft, compliant seal at temperatures ranging from 650 to 1000°C. These materials form excellent bonds to a variety of ceramics and metals during heating to the target operation temperature. They have limited reactivity with the fuel cell materials tested and are stable in both air and reducing environments.

Introduction

Sealant materials for high-temperature applications such as solid oxide fuel cells (SOFCs) must meet a number of requirements in terms of mechanical, chemical, and electrical properties. Basic requirements for a sealant are good bonding to the materials of interest, chemical stability in the operating environment, and low gas permeability. However, for high-temperature operation, the sealant must also have a thermal expansion which is reasonably close to that of the other materials involved and must have some compliance, or softness, to allow for some mismatch between the components to be joined. Material choices for such compliance are limited to soft glasses and, perhaps, ductile noble metals. However, only glasses have the potential for low cost as well as electrically insulating properties; thus, they are a reasonable sealant choice for the SOFC. In this paper, we discuss a family of glass-ceramic materials with mechanical, chemical, and electrical properties that are suitable for these demanding high-temperature applications.

No commercially available glass can act as a compliant high-temperature seal for long-term operation and can survive thermal cycling. Problems experienced by fuel cell manufacturers include chemical instability, inadequate viscosity at high temperature, and fracture during cooling due to thermal expansion mismatch. Proposed sealing materials include those based on soda-lime glasses [1], other alkali silicates [2], alkaline-earth silicates [2,3,4,5] and alkali borates (e.g., Pyrex [6,7]). Soda-lime glasses, such as Corning 0080, have suitably high coefficients of thermal expansion, CTEs (typically 9.5 × 10^{-6}/°C) for sealant use, but have unacceptably low viscosities at high temperatures (<10^3 Pa-s at 1000°C [8]). The alkali cations in alkali silicate and borate glasses also tend to be reactive at 1000°C. Alkali borate glasses such as Pyrex have undesirably low CTEs (3.2 × 10^{-6}/°C).

The ideal sealant from a mechanical standpoint would have a viscosity which changes slowly with changes in temperature (a low temperature index of viscosity) so that it is soft over a wide range of temperature, and yet has adequate viscosity at high temperature to form a stable

seal. Only below the glass transition temperature (T_g) is CTE matching important to minimize stress; above this temperature the sealant flows to accommodate mismatch strains. Our approach to developing a sealant with these properties was to start with a low-melting glass, with a T_g between 500 and 750°C, and to manipulate the temperature index of viscosity. The viscosity target was 10^6 Pa-s at the operating temperature. We also used known molar additivity coefficients developed by Appen (as discussed by Matveev et al. [9]) to choose a composition with the desired coefficient of thermal expansion in the temperature range below T_g.

We studied glasses based on boron oxide as the primary glass former to obtain a low T_g. We also studied glass-ceramics (SrO-La_2O_3-Al_2O_3-B_2O_3-SiO_2) to modify the viscosity behavior. Two of the other constituents of the sealant were the same as those in SOFC materials, strontium and lanthanum oxides. All added constituents serve distinct purposes: strontium oxide was added to increase the CTE of the glass [9,10]; lanthanum oxide was added primarily to modify/control the viscosity of the glass [9]; and alumina was added to retard crystallization of strontium borate and other crystalline phases (since it is known to inhibit devitrification of borates and silicates [11,12,13]). Small amounts of silica were added, primarily, to enlarge the glass-forming composition range with these constituents, but silica also increases the softening temperature and increases the viscosity of borate-based glasses.

Experimental

Materials preparation. Reagent grade $Sr(NO_3)_2$, La_2O_3, Al_2O_3, H_3BO_3, and SiO_2 were combined in the desired molar ratios and ground together in methanol in a vibratory mill to achieve a homogeneous mixture. The resulting powder was dried and then calcined at 800°C for 12 h. Calcined powders were then placed in platinum crucibles, heated to 1400°C, and held for 30 min. Small batches (30 g) were removed from the furnace and quickly poured from the crucibles into graphite molds. Larger, commercial-scale batches (2-4 kg) were made by discharging the melt from a hopper into water-cooled steel rollers, producing 1-mm-thick flakes of the material. The cooled glasses and glass-ceramics were reduced to a fine powder (5-15 μm) by using either mortar and pestle or vibratory mill. These powders were either uniaxially pressed, slurry-coated, or tape-cast to provide samples for characterization and for bonding tests.

To make bars for dilatometry or viscosity measurement, 20 g of the material was first pressed into a 6.35-cm-dia disk and heated to 1000°C for 6–12 h. Rectangular bars, approx. 3–5 cm × 0.4 cm × 0.4 cm, were cut from this disk and polished. The slurry-coating pastes consisted of a 75:25 wt % powder:glycerol mixture. When applied to the substrates, test samples were heated to 1000°C in air for 6 h.

Tapes of the sealant materials were made using commercial binders, plasticizers, and dispersants. Typically, 40 g of the sealant powder, 10 g of AT-51 binder [Rohm and Haas], 2.5 g of Santicizer 160 [Monsanto], 2 g of Solsperse 9000 [Monsanto], and 16 g of solvent (78:22 vol% xylene:butanol) were blended and cast using standard doctor-blade techniques. The tapes were allowed to dry slowly in air. Such tapes were used to make gaskets for test cells by first pre-shrinking them at 800°C for 6 h on a platinum foil, followed by assembling the cell and heating to 1000°C for 6 h in air.

Characterization. The crystalline phases present in the glass-ceramic materials were determined by X-ray diffraction (XRD, Phillips diffractometer). For microstructural determination, samples of the sealant and composite structures were mounted in epoxy and polished. A scanning electron microscope (SEM, JEOL JSM-35) along with energy-dispersive analysis of X-rays (EDAX) was used to examine the microstructure and determine approximate compositions of the amorphous and crystalline phases present.

Thermal expansion data were obtained from polished bars of annealed specimens in a Netsch dilatometer. Heating rates of 2°C/min were used. Glass-transition temperatures (T_g) of the glasses in the solid bars were determined by observing abrupt slope changes in plots of the dilatometric data. These temperature were checked against viscosity-based T_g calculations, as well as data from differential thermal analysis (DTA, Netsch STA 409).

Viscosities of the sealant materials were determined by the bending-beam method [14,15] in the temperature range of 600–1000°C. In this method, the sagging of rectangular bars of the sealant materials versus time at the test temperature is measured. For a simply-supported beam loaded with a weight at the center, the viscosity is given by:

$$\eta = \frac{gL^3}{2.4\ I_c\ (\frac{ds}{dt})}[\ M + \frac{\rho AL}{1.6}\ ] \qquad (1)$$

where η is viscosity (poise; 10 poise = 1 Pa-s), g is the acceleration due to gravity (cm/s^2), L is the support span (cm), I_c is the cross-section moment of inertia (cm^4), ds/dt is the rate of sag of beam at its midpoint (cm/min), M is the mass centrally applied to beam (g), ρ is the density of the beam (g/cm^3), and A is the cross-section area of the beam (cm^2). In our tests the beams were allowed to sag under their own weight, i.e., M was zero. The ρAL term is the mass of the beam itself (M_b). The cross-section moment of inertia, I_c, for a rectangular bar geometry equals $bd^3/12$ [16], where b is the beam width (cm) and d is its depth (cm). Equation (1) then simplifies to:

$$\eta = \frac{3.1\ M_b\ gL^3}{(\frac{ds}{dt})\ bd^3} \qquad (2)$$

Viscosity values obtained with this equation were extrapolated to low temperatures, where a value of 10^{13} Pa-s was used as a T_g indicator to check against other T_g data.

The gas permeability of these glasses and glass-ceramics was checked by measuring their ability to maintain oxygen pressure gradients. Simple oxygen concentration cells (see Fig. 1) were constructed by using the most promising sealant materials as gasket seals. Tapes of sealant material were cut into 'O'-rings, pre-shrunk at moderate temperatures (for example, 800°C) and bonded to thick-walled, open-ended tubes of Coors ZDY-4YSZ by heating to 1000°C. Platinum paste electrodes were applied to both sides of a 500-μm-thick disk of yttria-stabilized zirconia (YSZ). In the tests conducted at 800–1000°C, humidified helium gas containing 6% H_2

provided an oxygen partial pressure of 10^{-19} atm, and the furnace air outside provided an oxygen partial pressure of 0.21 atm. Cell voltages were measured with a digital multimeter (Hewlett-Packard 3467A). To determine the permeability of oxygen through the sealant gasket, the flow of hydrogen was periodically shut off. The resulting rate of EMF change was used to calculate the oxygen permeation constant, K [17]:

$$K = \frac{RT}{4F} \left(\ln \frac{(p_1 - \Delta p_1)}{p_1}\right) \frac{d}{A\ t\ (p_1 - p_2)} \qquad (3)$$

where R is the gas constant, T is temperature, F is Faraday's constant, A is the area through which permeation can occur, t is time (in seconds), p_1 and p_2 are the internal and external oxygen partial pressures, and d is the permeation distance.

The chemical stability and bonding behavior of these materials were determined by thermal cycling, followed by characterization of microstructure and weight loss. The sealant was fired alone or in layered structures composed of the sealant with various materials. Tests were done between room temperature and 1000°C over a range of oxygen partial pressures.

Results and Discussion

Structure. We tested more than 40 compositions in our five-component oxide system. Some 20 of these were glasses and glass-ceramic materials. Details of the observed glass-forming regions are reported elsewhere [18]. We were able to predictably alter compositions to obtain a desired ratio of glass to crystalline material. Two specific compositions, Materials 14 and 43 (a glass-ceramic and a glass, respectively) were eventually chosen as exemplary sealing materials. Scaleup of batch sizes for these materials resulted in an increase in the glass-to-ceramic ratio, probably due to the more rapid quench from 1400°C. Experiments continue to determine what changes in composition and heating schedule are necessary to compensate for differences in the two production techniques.

Crystallization could usually be determined with the SEM by the observation of faceted precipitates in the glass matrix. X-ray diffraction showed that the as-quenched materials contained the high-temperature phase of $LaBO_3$, while ground and sintered samples contained the low-temperature phase of this compound [19]. In both cases, about 5% strontium content was detected in the crystalline material. Diffuse peaks from the glass regions were also present.

Thermal Expansion. According to the rules of Appen (as discussed by Matveev et al. [9]), in order to attain a CTE between 8 and 12 × 10^{-6}/°C, the sealant should consist of 5–60 mol% SrO, 0–45 La_2O_3, 0–15 Al_2O_3, 15–80 B_2O_3, and 0–40 SiO_2. Within this composition range, we found thermal expansions ranging between 7 and 16 × 10^{-6}/°C. Pure glasses had expansions in the 8 to 9 × 10^{-6}/°C range, while glass-ceramics had higher expansion coefficients.

Linear regression analysis was performed on the expansion data to determine first-order

effects from the variations in composition. For simplicity, pure strontia was used as the y-intercept, since strontia has the highest thermal expansion of the five pure components (12.5 $\times 10^{-6}$/°C). Lanthana, alumina, silica, and boria percentages were used as independent variables. The best fit gave an intercept of 13 $\times 10^{-6}$/°C for pure strontia, while effects for addition of the other oxides were all slightly negative, with coefficients ranging from -0.01 for lanthana to -0.04 for alumina. Higher-order analyses failed to significantly improve the fit. The most convenient way to control the thermal expansion, then, is the strontia content, while the next most effective change is the alumina percentage. Other considerations, such as the viscosity behavior, will determine which substitutions are made.

Since the CTE depends, in part, on the amount of crystalline material present, devitrification over time at the service temperature is a concern. The effect of isothermal time at 1000°C on the CTE and microstructure was examined by heating bars of Material 14 to 1000°C and holding for times up to 120 h. Figure 2 shows dilatometry data from subsequent heating of bars which had been held at 1000 C for different times. These studies indicated no significant influence on the thermal behavior of the material where the material was rigid. The softening temperature remains unchanged, about 600°C. There are some changes in its expansivity in the temperature range where the glass in the material is soft, but these changes are not expected to affect its overall sealing properties. Comparing the microstructures of samples before the extended heat treatment with those after showed that the microstructure was unchanged.

Viscosity/Temperature Behavior. Beams of the glass and glass-ceramic materials sagged under their own weight when held at constant elevated temperature. The viscosities calculated from these experiments were found to obey log relationships with respect to temperature. Plots such as Figure 3 allow us to easily compare the various compositions for the desired softening characteristics. Again, a suitable sealant should have a viscosity of 10^6 Pa-s at operation temperature.

We found that, in terms of the 10^6 Pa-s criterion, pure glasses (Materials 42, 43, and 47) in our system tended to be suitable for 600 to 800°C operation, while glass-ceramics (Material K) tended to have viscosities suited for 800 to 1000°C operation. Materials 43 and 14 were determined to have the best combination of properties for use as sealants. Material 43 has a target operating temperature of 700°C and an extrapolated T_g (the temperatures at which the viscosity is about 10^{13} Pa-s [20]) of 560°C, while Material 14's corresponding temperatures are 1060°C and 660°C, respectively.

Evidence of T_g in dilatometer data for Material 14 is seen at about 600°C, where the slope of the curve reaches a maximum (Figure 2). Hence, there is fair agreement between these dilatometric T_g's and the viscosity-derived T_g.

That glass-ceramics have higher viscosities and flatter slopes with respect to temperature than pure glasses is not surprising; even though the glass matrix softens at a low temperature, the second phase keeps the viscosity of the sintered material high and suitable for use at 1000°C.

Bonding Behavior. Pastes and tapes of Materials 14 and 43 yielded extremely adherent and mechanically durable bonds to coupons of yttria-stabilized zirconia (YSZ), NiO/YSZ, and

strontium-doped lanthanum manganite. Materials 14 and 43 softened enough to form strong bonds at 1000°C and 650°C, respectively. Substrate/sealant composites in a variety of geometries were thermally cycled between room temperature and 1000°C to gauge the thermal compatibility of the sealant with the substrates. No delamination was observed. Structures with sealant between combinations of fuel cell anodes, cathodes, and electrolytes (which have slightly different CTE's) were also thermally cycled up to 10 times in humidified helium with 5% H_2. No cracking was observed in these structures.

Because of the bonding process, some interdiffusion of cations occurs between the sealant and substrate. Tapes of Material 14 were fired in contact with 100-μm-thick coupons of YSZ, nickel-zirconia cermet, and strontium-doped lanthanum manganite for 96 h at 1000°C to examine the extent of interaction. Interaction zones were observed with all substrate materials investigated. Examination of polished cross-sections in the SEM (see Figure 4) indicated that diffusion of elements from the substrate into the glass-ceramic occurred during bonding. If these materials are used in non-electrochemically active areas (such as at cell edges and stack-to-manifold junctions), this type of interaction may be acceptable.

Tolerance of up to a 20% mismatch in CTE values was demonstrated by sealing the cathode side of a monolithic SOFC structure to an alumina plate. After thermal cycling between room temperature and 1000°C, no cracking or delamination along the alumina/sealant or sealant/SOFC-cathode interfaces was seen. Examination of the alumina/sealant interface revealed that alumina had diffused into the sealant, producing an alumina-rich glassy phase. At the SOFC cathode/sealant interface, again, some diffusion of substrate ions into the sealant occurred. This diffusion may be responsible for a graded-CTE effect, akin to the graded-seal method used to join dissimilar materials with glass.

Stability. No significant changes were seen in these sealing materials when tested at high temperatures in air for long periods (up to 120 h). In humidified hydrogen, however, Material 14 had a small weight change, about 0.5%, in the first 6 h of exposure. The weight loss at first continued with additional exposure time; after a total exposure time of 120 h, weight loss was 0.9%. No further changes in weight were observed with longer times. Additional experiments were conducted to determine whether hydrogen or water alone could cause the weight loss. Neither exposure to water in helium carrier gas nor to pure hydrogen alone produced any significant weight change.

An X-ray diffraction pattern of the exposed surfaces of samples in which weight loss occurred indicated that no new phases formed, and composition changes could not be seen by using EDAX. Experiments continue to determine the volatile species, including wet chemical analysis and platinum cold-finger analysis of the furnace exhaust.

Gas Permeation. Oxygen concentration cells using Material 14 were tested in the temperature range 800–1000°C. Here, furnace air was the oxidant and flowing, humidified, 6% H_2 in He was the fuel. The cell EMF was measured at 800, 900, and 1000°C. All EMF's were 99% of the theoretical values calculated by the Nernst equation and were stable for periods of at least 3 days. During the test, the cell was thermally cycled between 400 and 1000°C five times and between room temperature and 1000°C once. The EMF's after thermal cycling stayed

within 1–2 mV of previous values. These experiments show that any gas leakage through the sealant is quite small in comparison to normal gas flow rates.

To quantify the permeation rate, simple measurements using Material 14 were made during the cell test at each of the three temperatures. For these measurements, the flow of gas was stopped, and the EMF was measured as a function of time. For calculation purposes it was assumed that the change in cell EMF was due solely to the permeation of molecular oxygen through the seal; since other sources of leakage are possible, this should provide an upper limit to the sealant permeation coefficient. The calculated values of K (in mm cm^3/s-cm cm-Hg) ranged from 2×10^{-23} at 800°C to 5×10^{-17} at 1000°C, and did not change with thermal cycling. These values are comparable to those of vitreous quartz [11], and we can conclude that our materials are excellent sealants with respect to oxygen permeation.

Conclusion

Our glass-ceramic materials appear to have a suitable combination of properties for high-temperature applications such as SOFCs. Their low glass transition temperatures and low temperature index of viscosity lead to a wide temperature range in which the sealant is soft yet mechanically stable. Accommodation of large CTE mismatches has been demonstrated. The sealant CTEs have been tailored to desired values for matching to a variety of ceramic and metal components within the low-temperature range when the sealant is rigid. Finally, it has been shown that their stability and gas permeability are suitable for applications in which gases with widely varying oxygen partial pressures must be separated for extended periods of time.

Acknowledgments

The authors thank Ben Tani of the Analytical Chemistry Laboratory for performing the X-ray diffraction analyses and Mark Hash of the Advanced Battery Group for performing the thermal analyses. This work was done under the auspices of the U. S. Department of Energy, Morgantown Energy Technology Center, under contract number W31-109-Eng-38.

References

1. Harufuji, Y., Jpn Kokai Tokkyo Koho JP 04-280,077 (Oct. 6, 1992).
2. Phillips, S.V., Datta, A.K., and Lakin, L., **Proc. Int. Symp. Solid Oxide Fuel Cells, 2nd**, 2-5 July 1991, Athens, Greece, pp. 737-745.
3. Stolten, D., Monreal, E., and Müller, W., **Fuel Cell Seminar Abstracts**, Nov. 29-Dec. 2, 1992, Tucson, AZ, p. 253.
4. Späh, R.J., Zurell, K., and Koch, A., **Fuel Cell Seminar Abstracts**, Nov. 29-Dec. 2, 1992, Tucson, AZ, p. 257.
5. Mukaisawa, I., Jpn. Kokai Tokkyo Koho JP 06 60,891 (March 4, 1994).
6. Harufuji, Y., Jpn Kokai Tokkyo Koho JP 04-47,672 (Feb. 17, 1992).
7. Akiyama, Y., Ishida, N., Murakami, S., and Saito, T., US Pat. No. 4,997,726 (March 5, 1991).
8. **Materials for the Design Engineer: Properties of Corning's Glass and Glass-Ceramic Families**. Corning, Inc., Corning, NY, 1973.

9. Matveev, M.A., Matveev, G.M., and Frenkel, B.N., **Calculation and Control of Electrical, Optical, and Thermal Properties of Glass**, Ordentlich, Holon, Israel, 1975, pp. 14-31.
10. Volf, M.B., **Chemical Approach to Glass**, Glass Science and Technology, Vol.7, Elsevier, New York, 1984, p. 132.
11. Jean, J.H., and Gupta, T.K., J. Mater. Res., **8(2)** (1993) 356.
12. Jean, J.H., and Gupta, T.K., J. Am. Ceram. Soc., **76(8)** (1993) 2010.
13. Ohta, Y., Shimada, M., and Koizumi, M., J. Am. Ceram. Soc., **65(11)** (1982) 572.
14. Hagy, H.E., J. Am. Ceram. Soc. **46(2)** (1963) 93.
15. Strnad, Z., **Glass-Ceramic Materials**, Glass Science and Technology 8, Elsevier, New York, 1986, pp. 162-165.
16. Beer, F. and Johnston, Jr., E. R., **Mechanics of Materials**, McGraw-Hill, New York, 1981, pp. 579ff.
17. Kohl, W.H., **Handbook of Materials and Techniques for Vacuum Devices**, Reinhold Publishing Co., New York, 1967, pp. 10-13.
18. Ley, K. L., Meiser, J. H., and Bloom, I. D., to be published in J. Mater. Res.
19. International Centre for Diffraction Data, cards 12-762 and 13-571.
20. Rawson, H., **Properties and Applications of Glass**, Glass Science and Technology, Vol. 3, Elsevier, New York, 1980, pp. 74-82.

Figure Captions:

Figure 1. Diagram of oxygen concentration cell with glass-ceramic seal.

Figure 2. Thermal expansion behavior of bars of Material K which had been aged at 1000 C for different times.

Figure 3. Softening characteristics of glass and glass-ceramic materials in our system.

Figure 4. SEM micrographs and elemental distributions for sealant bonded to a) nickel-zirconia cermet (NZC), b) YSZ, and c) strontium-doped lanthanum manganite (LSM).

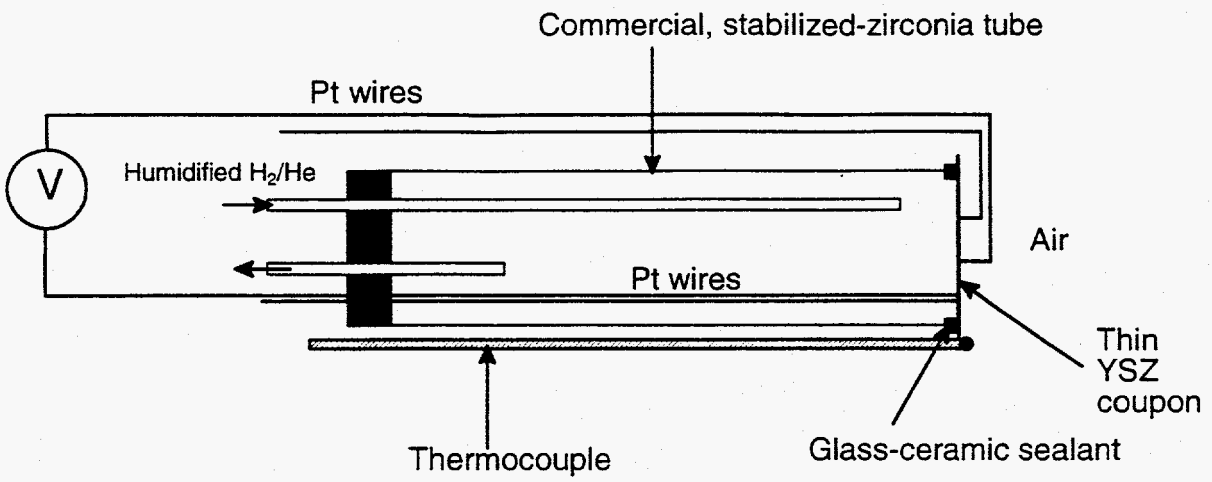
Commercial, stabilized-zirconia tube
Pt wires
V
Humidified H_2/He
Air
Pt wires
Thin
YSZ
coupon
Thermocouple
Glass-ceramic sealant

Fig. 1

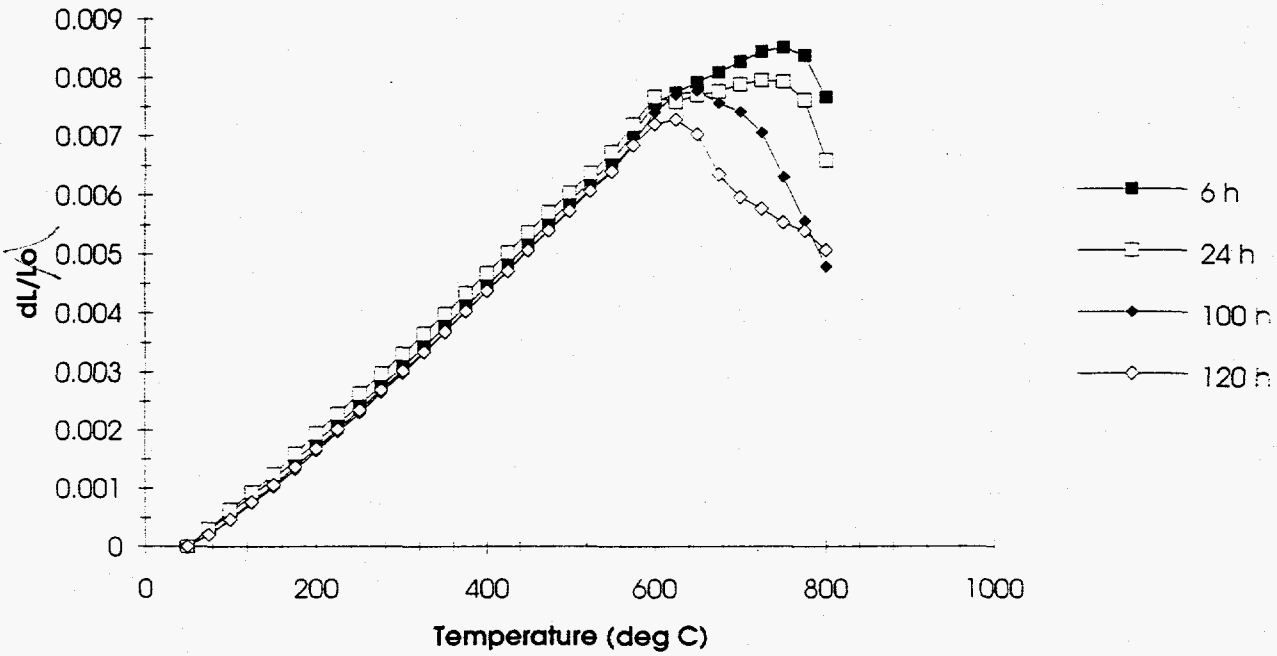

DISCLAIMER

Fig. 2.

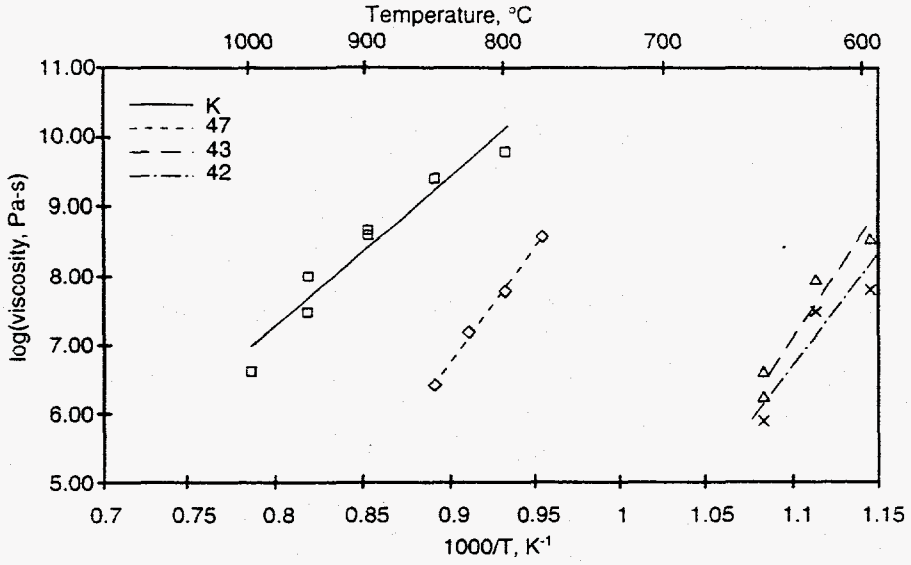
Temperature, °C
1000
900
800
700
600
11.00
10.00
9.00
8.00
7.00
6.00
5.00
log(viscosity, Pa-s)
K
47
43
42
0.7
0.75
0.8
0.85
0.9
0.95
1
1.05
1.1
1.15
1000/T, K-1

Fig. 3

Fig 4.

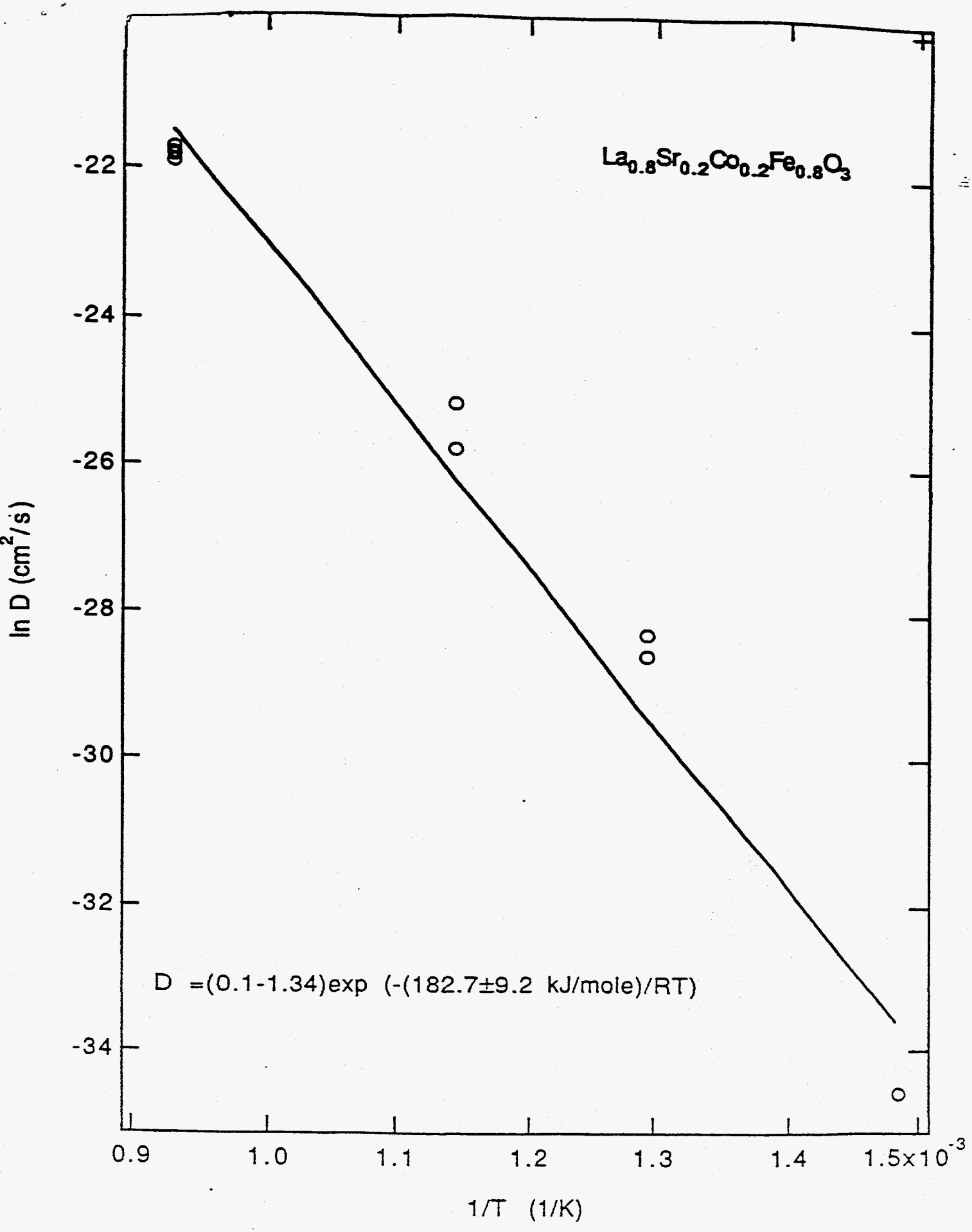

Fig. 4. Arrhenius plot of oxygen diffusion in $La_{0.8}Sr_{02}Co_{02}Fe_{08}O_3$